Supporting Information

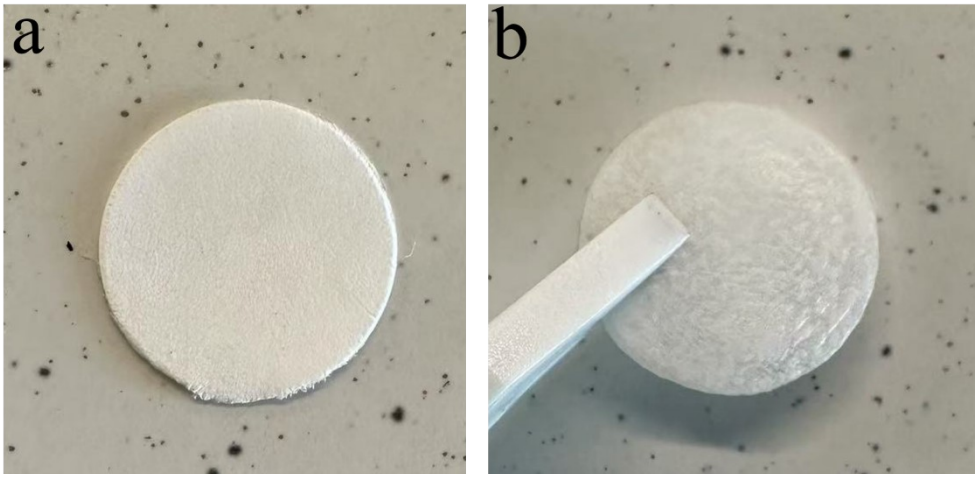

Figure S1. Optical images of HJ film a) before and b) after swollen with electrolyte solution.

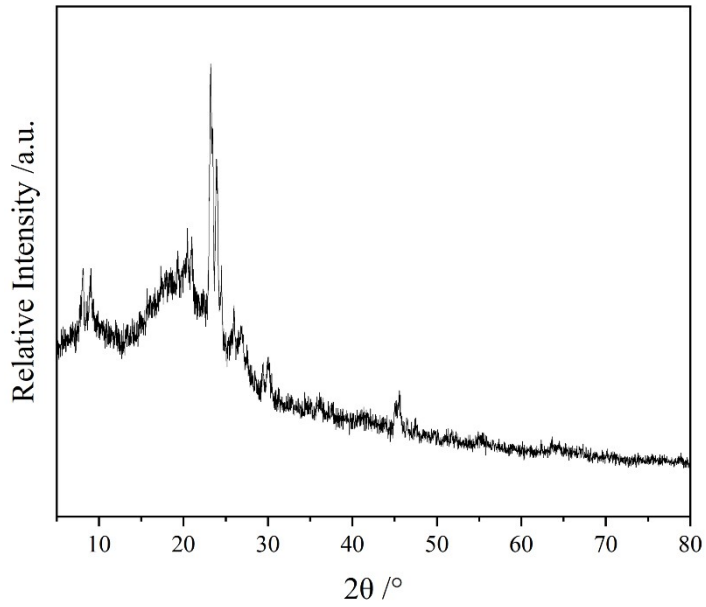

Figure S2. XRD pattern of a piece of HJ film.

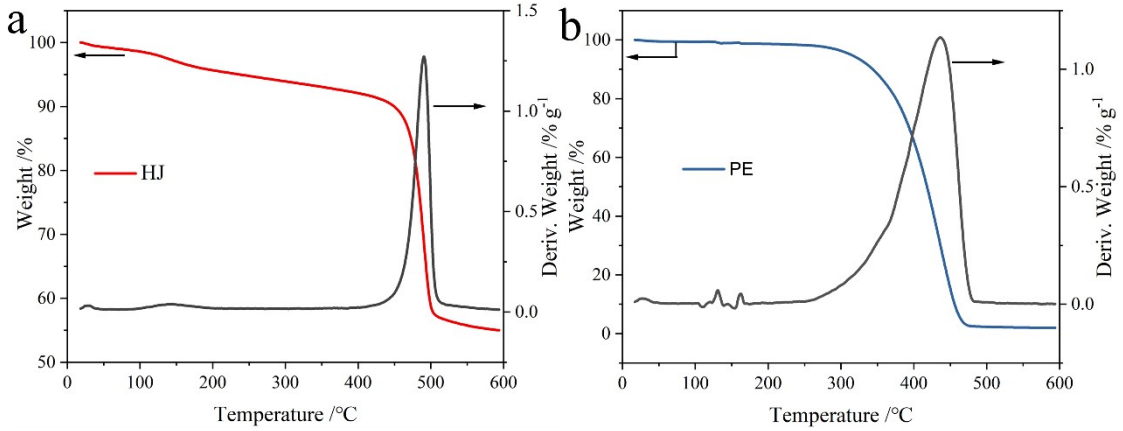

Figure S3. TG-DSC curves of a piece of a) HJ film and b) commercial PE film.

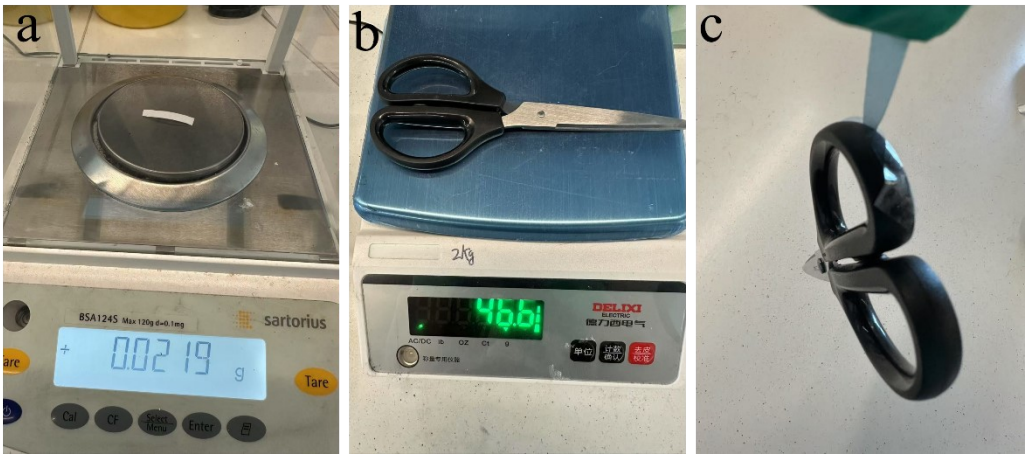

Figure S4. Weight of a) a piece of HJ film and b) load, c) picture of a piece of HJ film lifting a load.

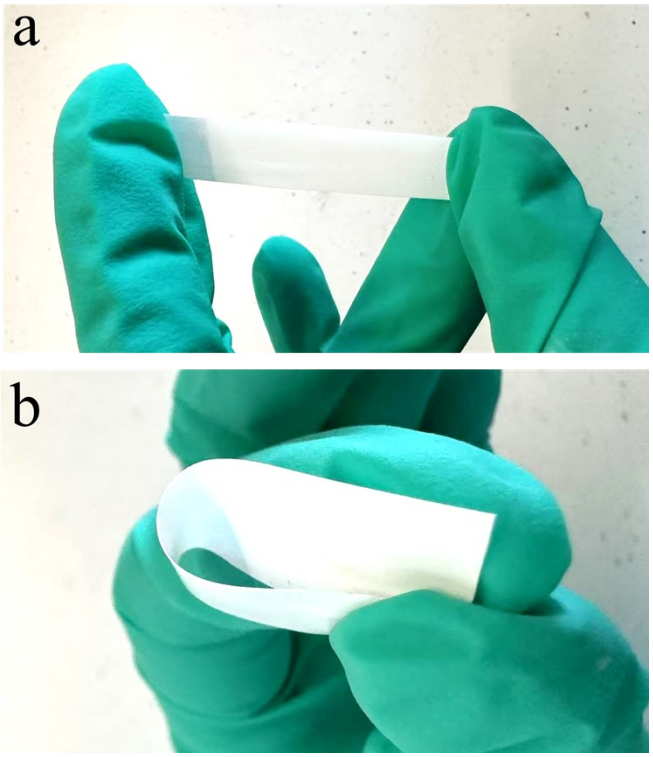

Figure S5. a) stretchability and bendability of the HJ film.

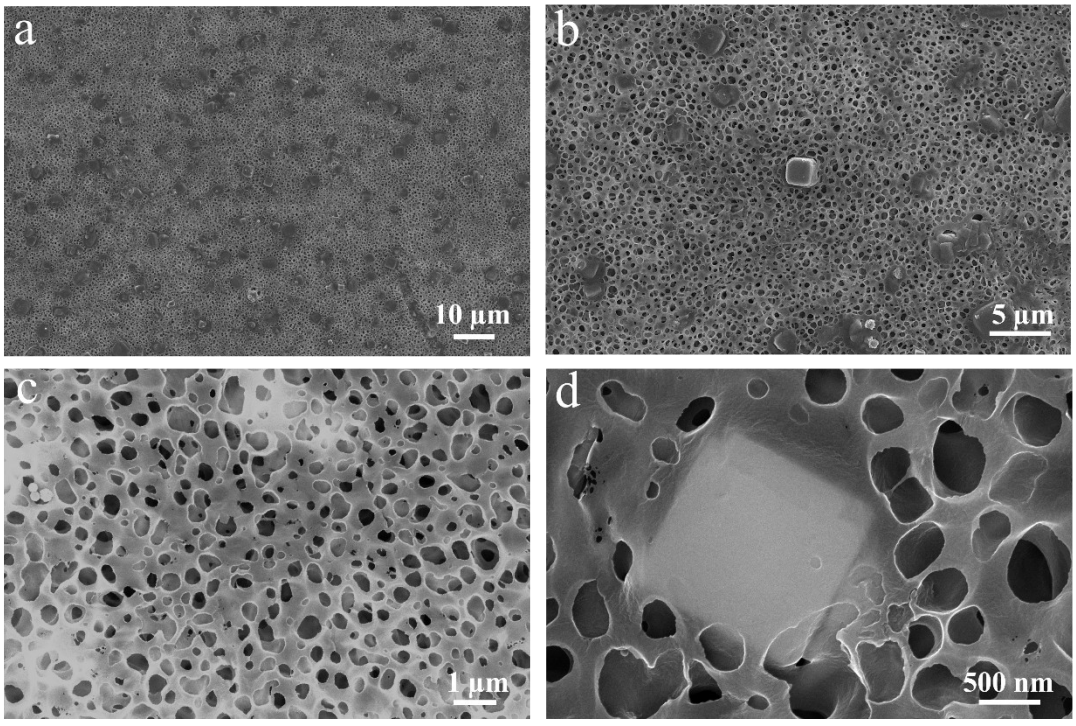

Figure S6. SEM images of HJ film (front side) synthesized with a lower ratio of DI water (400 mL).

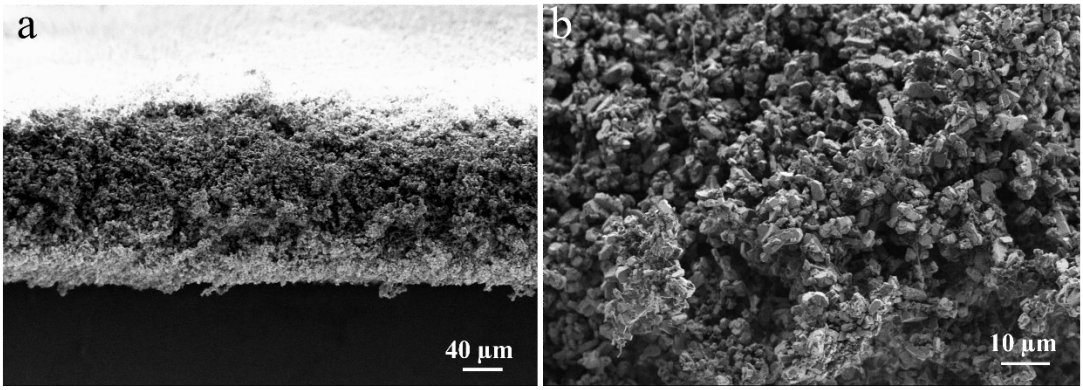

Figure S7. SEM images of the ZSM-5/PVDF-HFG film with an increased ratio of 9:1.

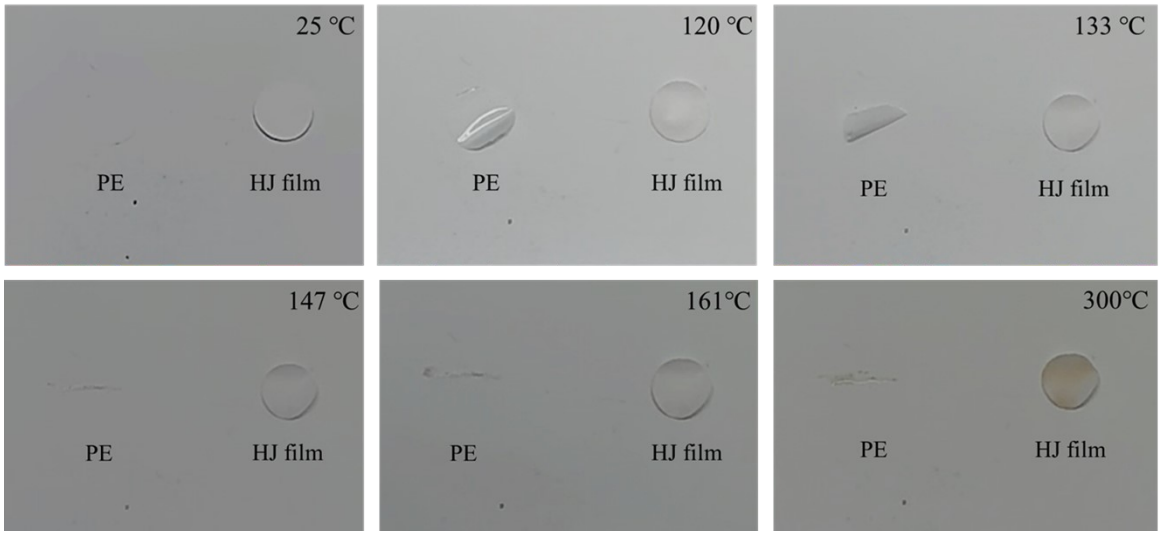

Figure S8. Thermal stability of PE and HJ film.

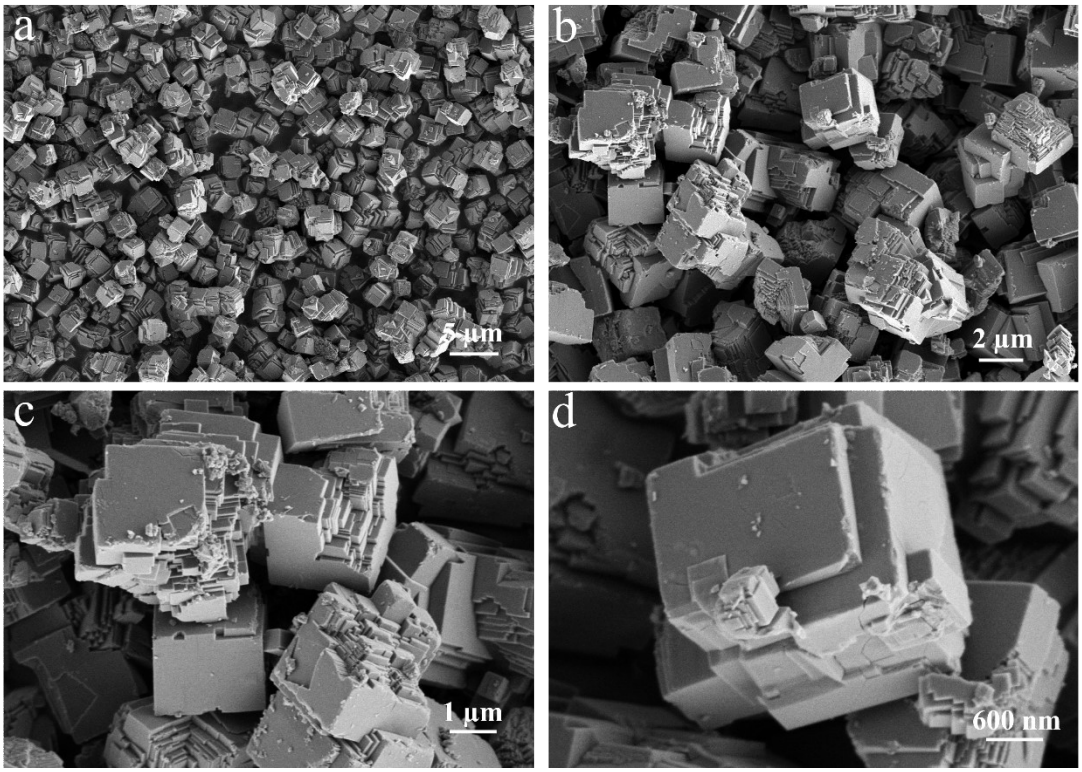

Figure S9. SEM images of PBAs with different magnifications.

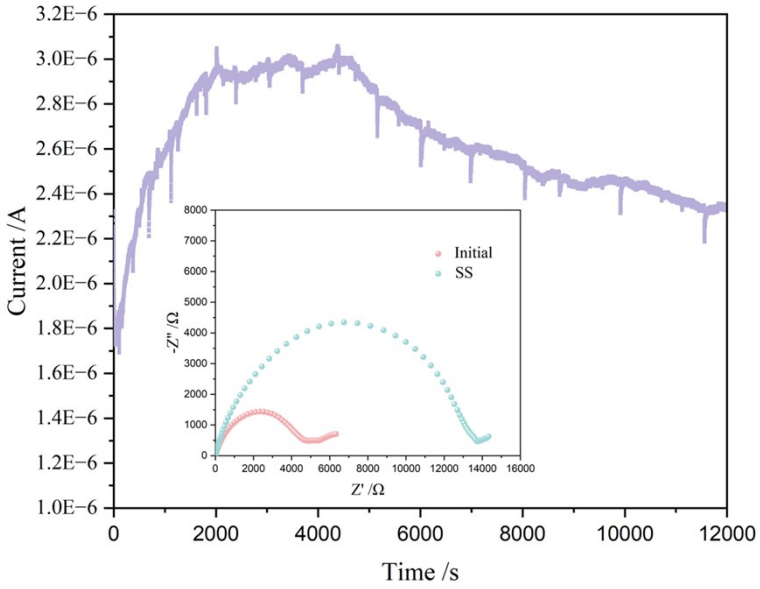

Figure S10. Steady-state current measurements and impedance spectra.

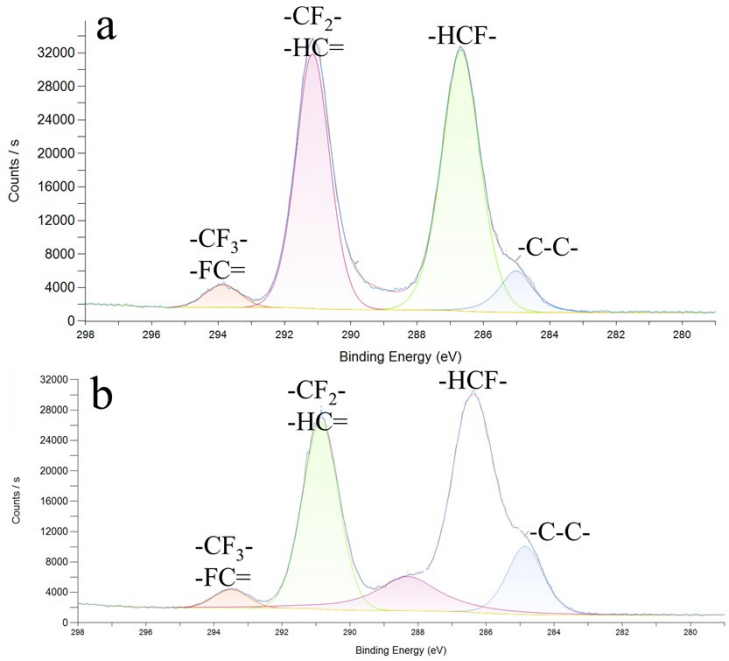

Figure S11. XPS tests. C1s spectra of HJ film a) before cycling and b) after cycling.

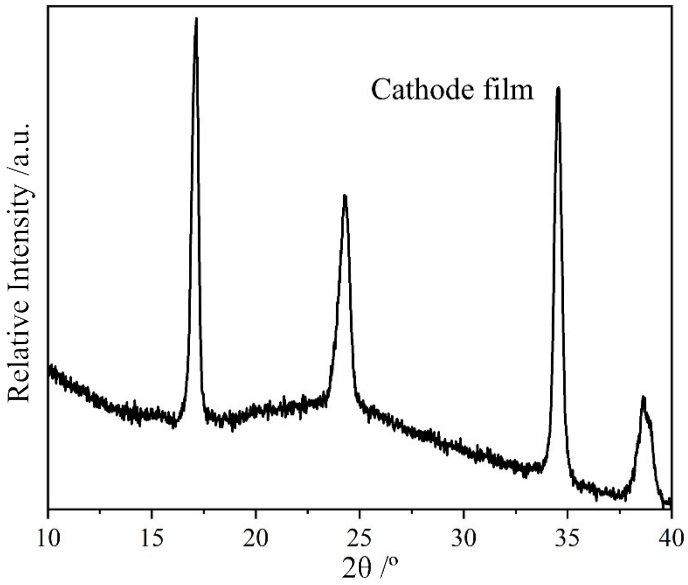

Figure S12. XRD pattern of a PBA-based cathode film (on Al foil).

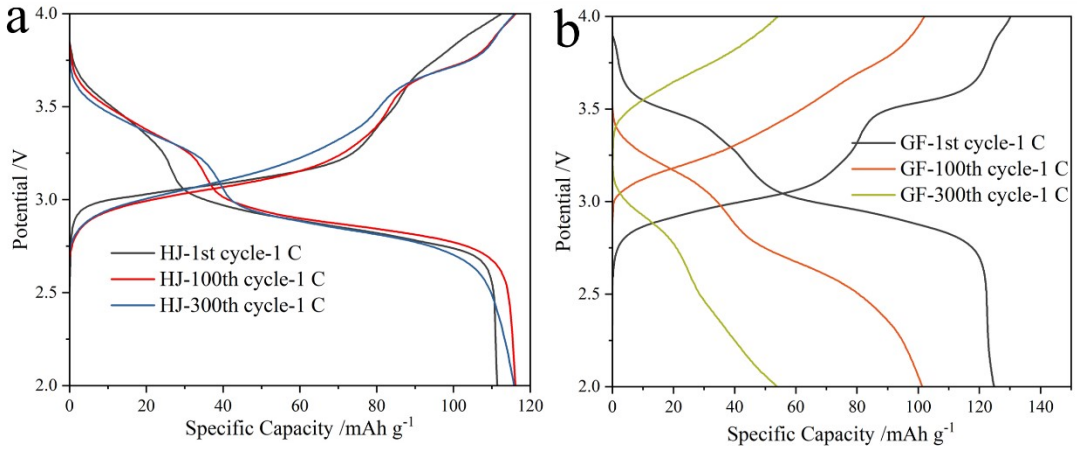

Figure S13. Charge-discharge curves of first, 100th and 300th cycle of a) HJ-based and b) GF-based sodium ion batteries.

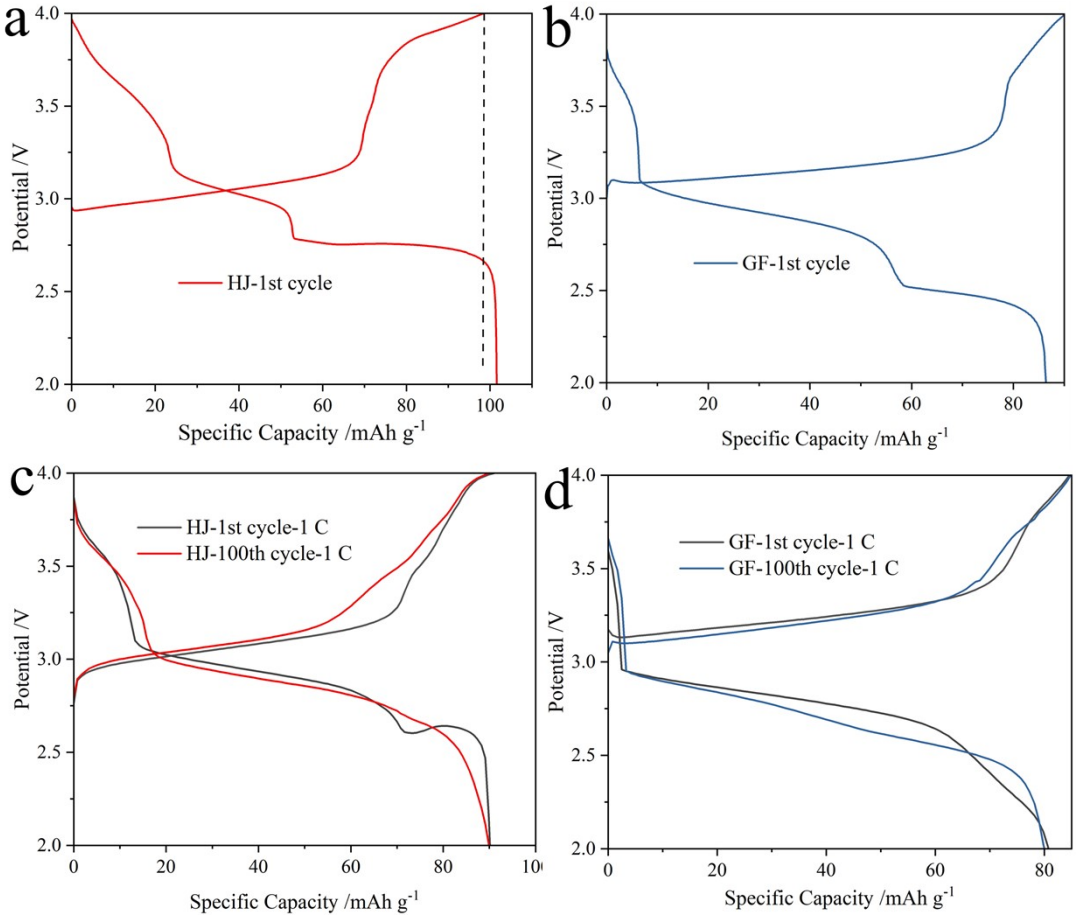

Figure S14. Initial charge-discharge curves of a) HJ-based and b) GF-based SIBs at 0.1 C at -20 ℃. First and 100th charge-discharge curves of c) HJ-based and d) GF-based SIBs at 1 C at -20 ℃.

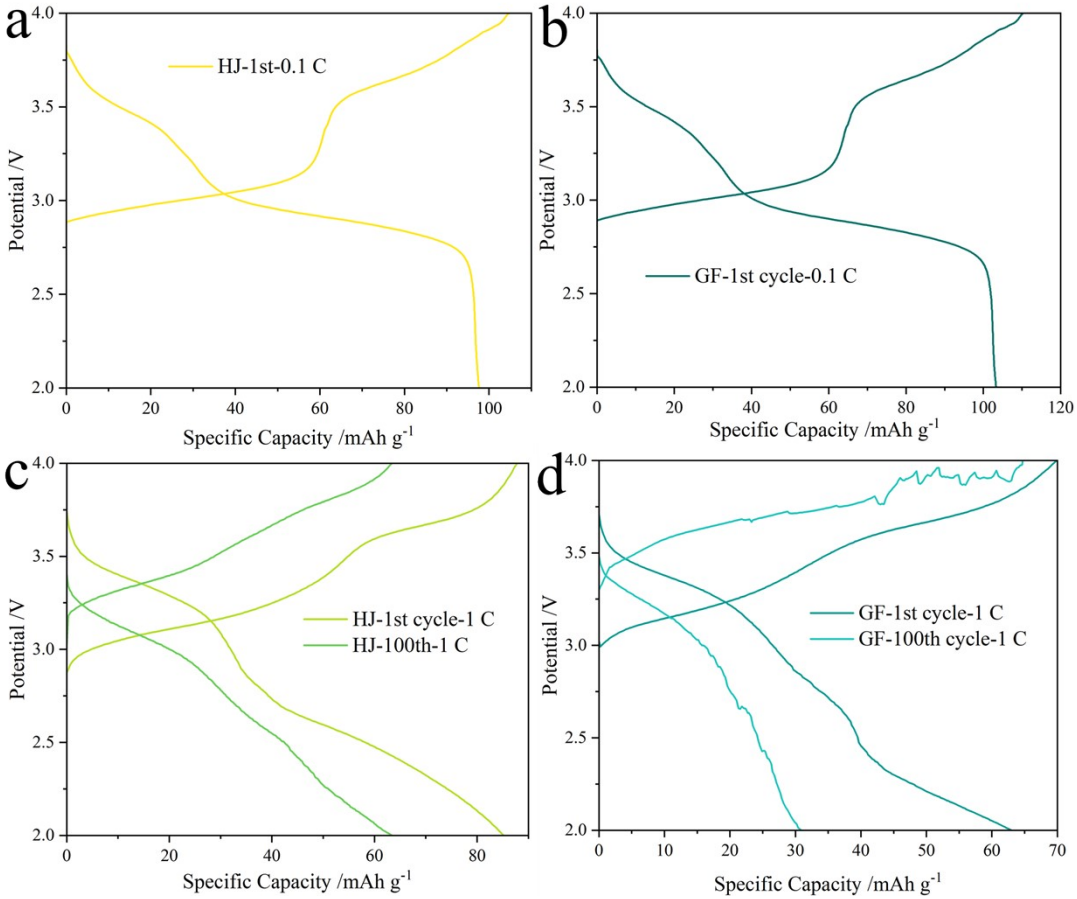

Figure S15. Initial charge-discharge curves of a) HJ-based and b) GF-based SIBs at 0.1 C at 60 ℃. First and 100th charge-discharge curves of c) HJ-based and d) GF-based SIBs at 1 C at 60 ℃.

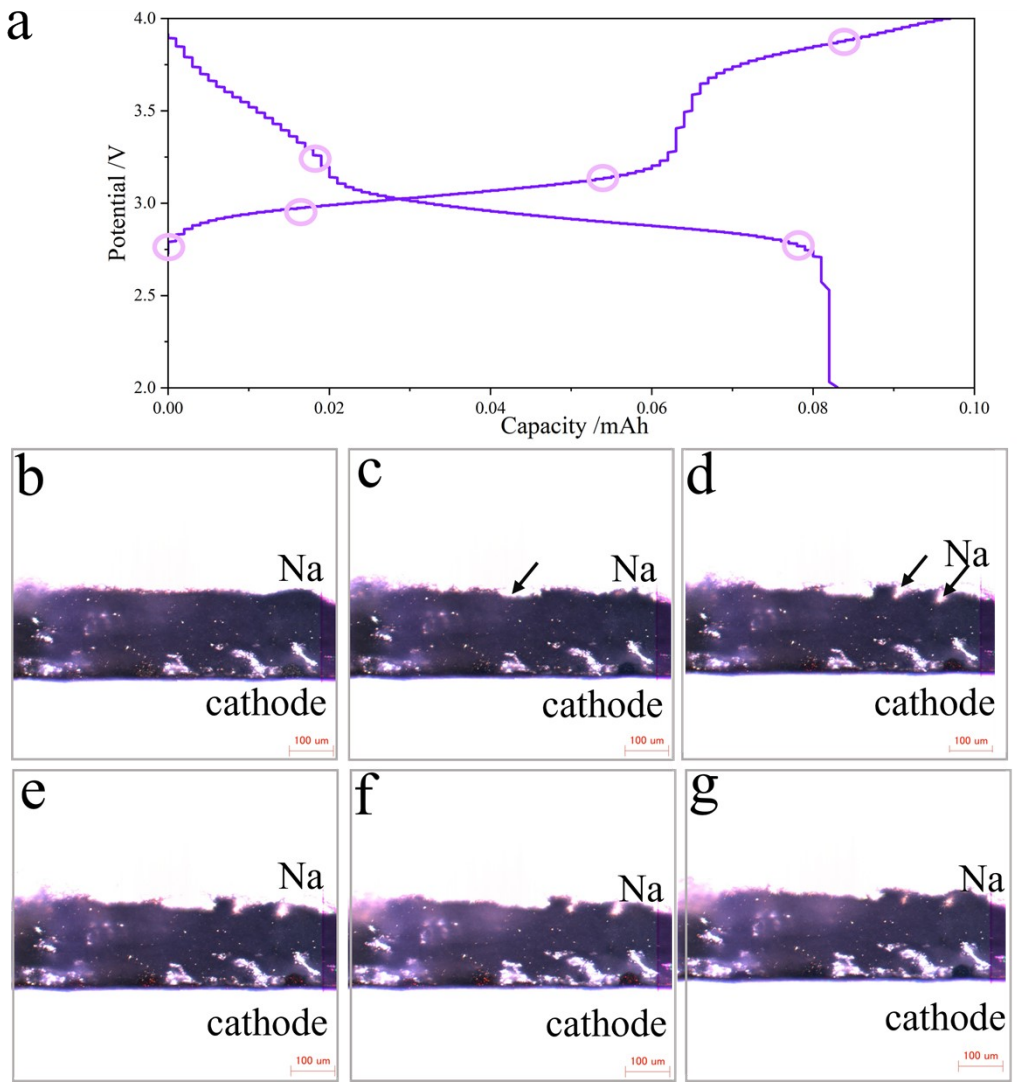

Figure S16. The process of evolution of the sodium metal growth. a) Charge-discharge curve of a full cycle. Operando confocal microscopic images of gel-state SIB a) at an initial state, b) charged to 3.0 V, c) charged to 3.1 V, d) charged to 3.8 V, e) discharged to 3.2 V and g) discharged to 2.8 V.